Absorption spectra, ligand field parameters and *g* factors of Cr^{3+} doped α-Al$_2$O$_3$ laser crystal: *ab initio* calculations

Emiliana-Laura Andreici Eftimie[1] and Nicolae M Avram[1,2]

[1] Department of Physics, West University of Timisoara, Bd. V. Parvan, No. 4, 300223, Timisoara, Romania
[2] Academy of Romanian Scientists, Independentei 54, 050094-Bucharest, Romania

E-mail: nicolae.avram@e-uvt.ro

CrossMark

Abstract

In this paper we present, in the unified frame, the results of the *ab initio* investigations of absorption spectra, ligand field parameters and *g* factors for three valence chromium doped α-Al$_2$O$_3$ crystal. Our calculations are based on a new methodology applied to a cluster [CrO$_6$]$^{9-}$ embedded in an extended point charge field of host matrix ligands. After the differential functional theory optimization of the doped crystal, a vibrational theoretical spectroscopic study based on infrared spectroscopy has been employed in order to confirm the stability of the optimized doped crystal structure. The *ab initio* energy calculation of the electronic states and corresponding wave functions of Cr^{3+} are documented from the complete active space self-consistent field. The improved energy states from the N-electron valence second order perturbation theory, second order dynamic correlation dressed complete active space (DCD-CAS2), difference dedicate configuration interaction with three degrees of freedom (MRDDCI3) and spectroscopy-oriented configuration interactions, were analyzed. Based on the *ab initio* ligand field theory procedure we extracted ligand field parameters and spin–orbit coupling constant which were used to recalculate the energy levels of the studied system. In addition, *g* factors for the ground state ^{4}A$_2$ of Cr^{3+} ion in corundum are calculated taking into account the full configuration interaction. The results obtained are discussed and the comparisons with measured values from literature show a reasonable agreement, which justifies and recommend this new route of investigation.

Keywords: Al$_2$O$_3$:Cr^{3+}, *ab initio* calculations, optical absorption spectra, ligand field, spin-hamiltonian parameters

(Some figures may appear in colour only in the online journal)

1. Introduction

Aluminum oxide (α-Al$_2$O$_3$- corundum) is the most stable phase of more than 15 distinct crystallographic phases of the Al$_2$O$_3$materials [1]. It possesses important physical properties such as high optical transparency, chemical and thermal stability, fine optical and dielectric characteristics, high refractive index, hydrophobicity, etc, [2, 3]. Due to these properties it has numerous technological applications such as laser hosts, sensors of the pressure and temperature, and others [4]. Also, having a large band gap ($\sim$8 eV) [5], corundum can act as a

tunneling barrier for organic transistors or novel magnetic sensors. The greatest bulk of α-Al$_2$O$_3$ crystals doped with transition metal (TM) ions such T^{3+}, V^{3+}, Cr^{3+} , etc, has wide applications in solid state laser devices [6–10]. There are many methods to prepare Al$_2$O$_3$:Cr^{3+} materials, such as the Czochralski method, sol-gel method, solid-state reaction, pulsed laser deposition, hydrothermal method and so on [11]. The energy levels of TM ions with the 3d^n (n = 1–9) configurations doped in different symmetry crystal sites have been the subject of both theoretical and experimental investigations previously [12–19]. The theoretical interpretations

of the experimental results have been done in the semi-empirical crystal field theory. In a pioneering paper, McClure [12] has investigated the polarized optical spectra of the Ti^{3+}, V^{3+}, Cr^{3+}, Mn^{3+}, Co^{3+}, Ni^{3+} ions doped in corundum single crystals, both from an experimental (at temperatures from 4.20 to 1200 K) and a theoretical point of view. He established the energy levels scheme of absorption spectra in the frame of point charge model of crystal field. Sturge [13], studied similar problems for V^{2+} ion doped in corundum single crystal at low temperature and Tanabe and Sugano [14] analyzed the absorption spectra of Cr^{3+} in ruby. The absorption spectra from excited state of Al_2O_3:Cr^{3+} material [15], the energy levels scheme of V^{2+}, Cr^{3+} and Mn^{4+} in octahedral crystal field [16] and the book [20] are some of the remarkable references that have studied the TM ions doped in α-Al_2O_3 crystal.

After 1990 mechanical quantum first-principle calculation of geometry optimization, band structure, density of states, charge density maps for Al_2O_3 crystal have been done, using Hartree–Fock method by Salasco and al., [21]. Nowadays in a recently published paper [17] the authors calculated the absorption spectra of α-Al_2O_3:V^{2+}, α-Al_2O_3:Cr^{3+}, and α-Al_2O_3:Mn^{4+} from first-principles configuration- interaction based on the discrete variational Xα method, taking into account the configuration-dependent correction and the correlation correction of the energies terms. M G Brik [18] produced a paper based on first-principles calculations of the structural and electronic properties of pure and Ti^{3+}-doped corundum at the ambient and elevated pressures.

Regarding the three valence chromium ion doped in different host matrices, the greatest effort was made on the Cr^{3+} ions doped in α-Al_2O_3 crystal. Cr^{3+} has electronic configuration $1s^22s^22p^63s^23p^63d^3$ and replaces, by doping, the Al^{3+} in distorted trigonal site, without charge compensation. Three valence chromium becomes the active element of the first laser -the ruby laser [22], which is still used worldwide. The chromium can absorb energy and reach the excited levels $^4T_2$ (the U band), $^4T_1$ (F) (the Y band) and $^4T_1$ (P) (the V band), resulting the absorption spectra [23]. This ion has strong absorption bands due to the electronic excitation from the ground state $^4A_2$ to excited states $^4T_2$, $^4T_1$ (F) and $^4T_1$ (P). Non-radiative transitions from these excited states to ^2E excited state take place, and the electron radiative transition from excited state ^2E to the ground state is followed by the characteristic luminescence at $\sim$694.3 nm (R-band) [23].

The aim of this paper is to investigate, in the unified frame, using the *ab initio* multireference methodology [24, 25], the absorption spectra, ligand field (LF) parameters and *g* factors for three valence chromium doped α-Al_2O_3 crystal. The method projects a new view on the connection between the optical and EPR spectra, regarding the local symmetry of the impurity ion, the covalence and the multiconfigurational interactions. Extracting the parameters of the ligand field from *ab initio* calculations and recalculating the absorption spectra of Cr^{3+} in a trigonal local symmetry, with the determination of the trigonal parameters, are new in the field. Moreover, we extend our work by including a brief analysis of the vibrational infrared (IR) spectra to certify the stability of the doped crystal structure after geometry optimization.

2. Methods of investigations

The single crystal α-Al_2O_3 belong to the R$\bar{3}$ c space group (No. 167 in the International Tables of Crystallography [26]), with the lattice constant $a = b = 4.7589$ Å, $c = 12.991$ Å, $\alpha = \beta = 90°$ and $\gamma = 120°$. The unit cell has two formula units with ten ions, 4 Al^{3+} at 12c and 6 O^{2-} ions at the 18 e Wyckoff positions, respectively (figure 1).

Each Al ion is coordinated by two groups of oxygen ions, and each such group consists of three ions located in the same plane perpendicular on the *c* axis of the crystal, on both sides of each aluminum's ion. The Al–O distances are 1.8570 Å in first group and 1.9729 Å in the second one, respectively. The geometry of α-Al_2O_3 from x-rays crystallography [28] was *ab initio* fully optimized with the CRYSTAL17 software [29]. The MO-LCAO approach, localized Gaussian basis set TZVP and the hybrid functional PBE0 [30], taking into account both local and nonlocal exchange, were used. The α-Al_2O_3 host crystal doped with Cr^{3+} was modelled by a $2 \times 2 \times 2$ supercell containing 80 atoms (figure 2), in which one of the 32 Al atoms was replaced by a Cr^{3+} ion, corresponding to 3.1%, a reasonable concentration of Cr^{3+} in corundum. The threshold of the self-consistent field (SCF) energy was set to 10^{-7}, the shrinking factor of the reciprocal-space net was set to 8 and for accelerating convergence we chose the Broyden scheme.

Based on the fully relaxed α-Al_2O_3:Cr^{3+} geometry, the $[CrO_6]^{9-}$ centered embedded cluster, which contains the central Cr^{3+}- and six coordinating O^{2-} ions, according to Gellé -Lepetit procedure [31] was built (for more details the readers are kindly invited to see the papers [24, 25]). In this cluster the Cr^{3+} ion is coordinated by two groups of oxygen ions, each of them having three oxygen ions, with the new distances Cr^{3+}–O^{2-} of 1.9402 and 1.9893 Å correspondingly, as a result of the optimization process. This quantum cluster (QC) is surrounded by a boundary region (BR) and both are embedded in a 'sea' of point charges (PC), according to the embedded cluster model [32] (figure 3).

Further, all calculations of optical and g factors on the $[CrO_6]^{9-}$ cluster were done with the ORCA 4.1 package [33] using the Douglas–Kroll–Hess Hamiltonian of 2nd order [34], with def2-TZVPP [35] basis set for all atoms. The effective core potentials for Al [SD (10, MWB)] [36], and O [SD (2, MWB)] [37] were taken from the pseudopotential library of the Stuttgart/Cologne group [38].

The 10 spin-quartets and 40 spin-doublet states of the three valence chromium ion, doped α-Al_2O_3, were calculated by complete active space self-consistent field (CASSCF) [39], NEVPT2 [40, 41] DCD-CAS2 [42], MRDDCI3 [43] and SORCI [44] methods. The same methods, with the effective spin-Hamiltonian and quasi degenerate perturbation theory (QDPT) approach [45] have been used to obtain the g factors The *ab initio* ligand field theory method (AILFT) [46] is a
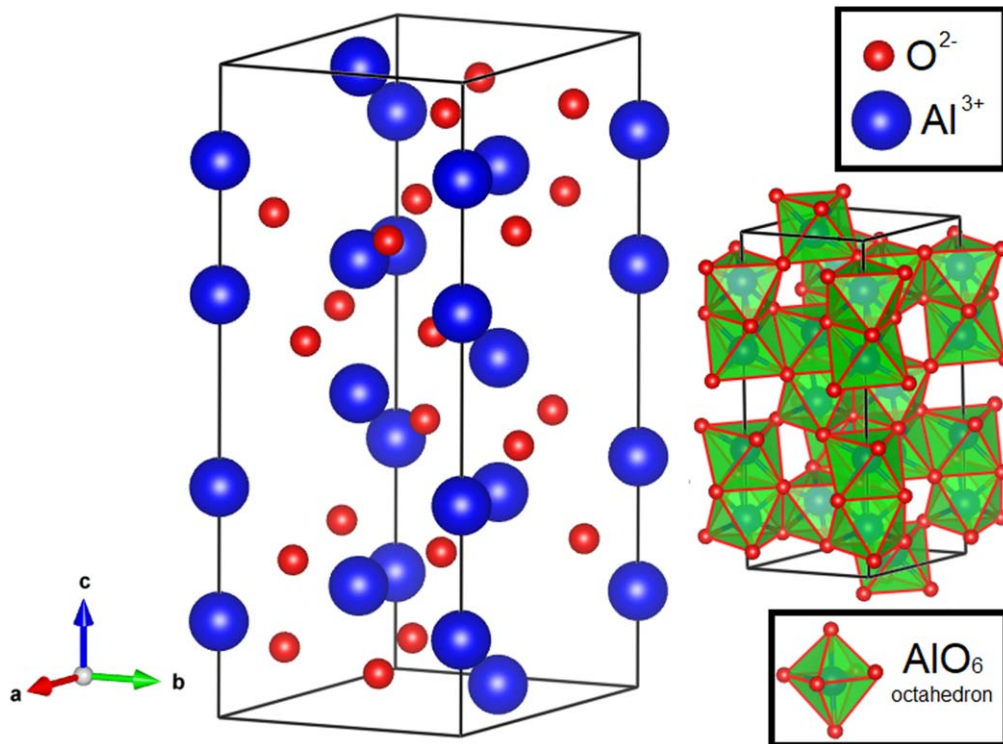
Figure 1. Unit cell of α-Al_2O_3 crystal (drawn with Vesta [27]).

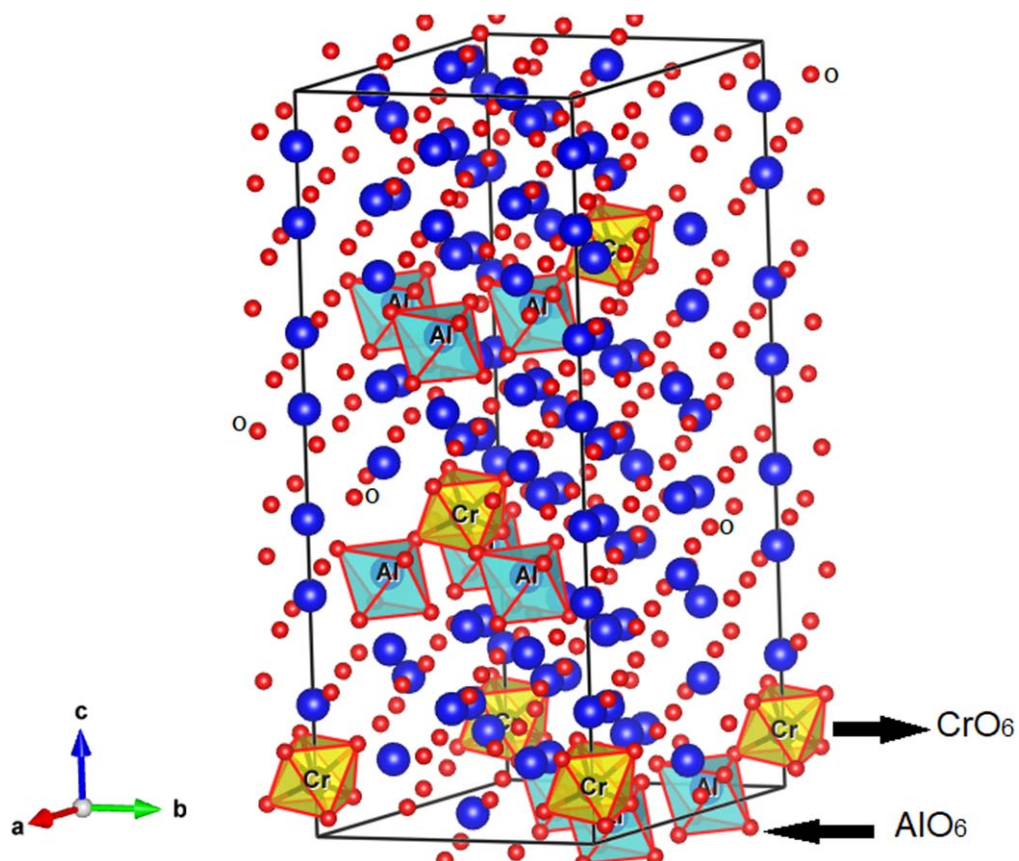**Figure 2.** $2 \times 2 \times 2$ supercell of α-Al_2O_3:Cr^{3+} (drawn with Vesta [27]).
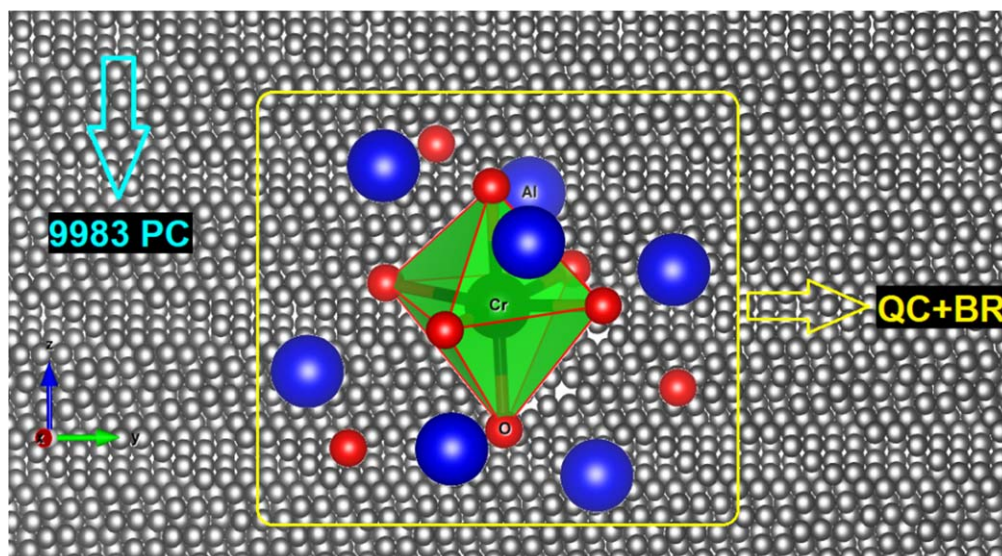
Figure 3. Embedded cluster model $[CrO_6]^{9-}$ (drawn with Vesta [27]).

Table 1. (a) Transition energies (cm^{-1}) between the ground state $^4A_2$ (^4F) and low lying excited spin-quartet states of α-Al$_2$O$_3$:Cr^{3+}. (b) Transition energies (cm^{-1}) between the ground state $^4A_2$ (^4F) and low lying excited spin-doublet states of α-Al$_2$O$_3$:Cr^{3+}.

Energy levels	Expt. [15]	CASSCF (3,5)	NEVPT2 (3,5)	CASSCF (7,12)	NEVPT2 (7,12)	DCD-CAS2 (0) (3,5)	DCD-CAS2 (1) (3,5)	SORCI (3,5)	MRDDCI3 (3,5)
(a)									
$^4A_2$(F)	0	0	0	0	0	0	0	0	0
^4E(F)	18 000	15 182	17 768	17 040	18 302	18 847	17 578	17 773	17 689
$^4A_1$(F)	18 400	15 596	18 351	17 487	18 865	19 434	18 139	18 437	18 034
^4E(F)	24 300	23 492	25 782	25 338	25 597	27 046	25 046	24 192	24 540
$^4A_2$(F)	25 100	24 485	26 688	26 241	26 311	28 016	25 933	25 039	24 016
^4E(P)	39 000	37 585	39 174	39 901	40 141	42 434	39 544	39 289	39 338
$^4A_2$(P)	39 200	37 612	39 709	40 018	40 775	42 929	40 082	40 220	39 070
RMS errors (cm^{-1}) →		1787.5	856.9	917.9	1015.5	2521.4	600.08	365.9	431.6
(b)									
^2E(^2G)	14 433	18 914	16 448	18 468	16 039	16 355	16 349	16 879	17 137
$^2A_2$(^2G)	15 063	19 843	17 342	19 306	16 758	17 340	17 245	17 706	16 807
^2E(^2G)	15 190	19 971	17 404	19 389	16 793	17 414	17 307	17 643	17 496
$^2A_1$(^2G)	20 993	27 263	24 789	26 715	24 117	25 275	24 475	23 630	23 596
^2E(^2G)	21 213	27 506	24 883	26 862	24 122	25 401	24 573	23 794	23 971
$^2A_1$(^2G)	29 425	31 085	31 595	32 445	31 626	32 411	31 361	31 721	31 602
RMS errors (cm^1)→		4578	2772	4612	2229	3069	2571	2502	2473

powerful tool which allows us to extract ligand field parameters and effective spin–orbit coupling constant of a transition metal doped into a complex, for the case of minimal complete active space. From the splitting of quartet electronic states it is also possible to calculate the trigonal ligand field parameters v and v'. According to [47] the absolute values of the orbital triplet-states splitting are: $^4T_2$: $v/2$; $^4T_1$ (F): $v/2+v'$; $^4T_1$ (P): $v–v'$. Comparison of these expressions with the results from *ab initio* calculations gives the approximate values for the trigonal crystal field parameters. It should be pointed out that the values of these parameters, together with those obtained directly from AILFT procedure, serve to re-calculate the LFT spectra [48, 49] and to analyze the

covalence effects in the presence of ligands [50]. The obtained results after each step of calculations, in the frame of the above-presented methods, were analyzed and comparison between those and measured data were carried out.

The IR spectra of α-Al$_2$O$_3$:Cr^{3+} were simulated using the CRYSTAL17 software [29] in harmonic approximation, in center of the first Brillouin zone, at Γ point, in order to point out the normal modes of vibration belonging to Al–O and Cr–O stretching bonds and the reliability of the doped crystal.

Table 2. Trigonal ligand field (cm^{-1}) of α-Al$_2$O$_3$:Cr^{3+}.

Trigonal parameters	Expt. [15]	CASSCF (3,5)	NEVPT2 (3,5)	CASSCF (7,12)	NEVPT2 (7,12)	DCD-CAS2(0) (3,5)	DCD-CAS2(1) (3,5)	SORCI (3,5)	MRDDCI3 (3,5)
v	800	820	1160	890	1110	1170	1100	1300	700
v'	680	800	630	760	500	670	580	410	500

E-L Andreici Eftimie and N M Avram

Table 3. g factors calculated with the QDPT procedure.

Parameter	Expt. [51]	CASSCF (3,5)	NEVPT2 (3,5)	CASSCF (7,12)	NEVPT2 (7,12)	SORCI (3,5)	MRDDCI3 (3,5)	HF
g_{iso}	1.97	1.964	1.969	1.970	1.973	1.973	1.971	1.971

Table 4. AILFT ligand field parameters and spin–orbit constant (cm^{-1}).

Method (3,5)	Dq	B	B_0	C	C_0	Dq/B	C/B	C_0/B_0	ξ	ξ_0
CASSCF	1514	1025	1159	3856	4336	1.48	3.76	3.74	254.9	277.9
NEVPT2	1544	960	997	3122	3873	1.61	3.25	3.89	—	—
DCD-CAS2(0)	1860	887	1024	3442	3989	2.10	3.88	3.90	—	—
DCD-CAS2(1)	1729	813	981	3416	3953	2.13	4.20	4.03	—	—
Expt.[51]	1779	683	918[a]	3110	3850[a]	2.75	4.55	4.19[a]	—	273[a]
Expt.[15]	1815	645	918[a]	3000	3850[a]	2.81	4.65	4.19[a]	—	273[a]

[a] [52].

Table 5. (a) Transition energies (cm^{-1}) between the ground state $^4A_2$ (^4F) and low lying excited spin-quartet states of α-Al_2O_3:Cr^{3+}, calculated with parameters from AILFT method. (b) Transition energies (cm^{-1}) between the ground state $^4A_2$ (^4F) and low lying excited spin-doublet states of α-Al_2O_3:Cr^{3+} calculated with parameters from AILFT method.

Energy terms	LFT (CASSCF)	LFT (NEVPT2)	LFT (DCD-CAS2 (0))	**LFT (DCD-CAS2 (1))**
(a)				
$^4A_2(F)$	0	0	0	0
$^4E(F)$	15 002	15 292	18 389	17 095
$^4A_1(F)$	15 381	15 687	18 946	17 607
$^4E(F)$	23 257	23 366	26 729	24 773
$^4A_2(F)$	24 237	24 301	27 713	25 681
$^4E(P)$	37 194	36 985	41 888	38 848
$^4A_2(P)$	37 271	37 158	42 433	39 336
RMS errors (cm^{-1}) [a] $\rightarrow$	279.7	2423.7	447.5	526
RMS errors (cm^{-1}) [b] $\rightarrow$	2006.4	1915.7	2153.1	558.2
(b)				
$^2E(^2G)$	18 615	15 978	16 607	16 034
$^2A_2(^2G)$	19 583	16 938	17 486	16 817
$^2E(^2G)$	19 700	17 030	17 555	16 885
$^2A_1(^2G)$	26 858	23 568	25 056	24 072
$^2E(^2G)$	27 084	23 745	25 148	24 172
$^2A_1(^2G)$	30 802	28 641	32 456	30 778
RMS errors (cm^{-1}) [a] $\rightarrow$	104	1233	202	417
RMS errors (cm^{-1}) [b] $\rightarrow$	4750	1975	3040	2180

[a] Reference energies.
[b] Experimental energies.

3. Results and discussions

The free three valence chromium ion has, in the LS coupling scheme, 8 lS terms: ^4F, ^4P, ^2P, $^2D_{1, 2}$, ^2F, ^2G, ^2H, with the ^4F term as the ground term. These terms are split by crystal field, with octahedral symmetry of host matrix, according to group symmetry rules. The orbital ground term ^4F is split into the orbital singlet $^4A_2$ (the ground state) and two orbital triplets $^4T_2$ and $^4T_1$ (F). The excited quartet ^4P term is not split by the cubic crystal field, he is displaced, giving the second $^4T_1(P)$ state. The absorption spin-allowed transitions $^4A_2 \rightarrow {}^4T_2$, $^4A_2 \rightarrow {}^4T_1$ (^4F) and $^4A_2 \rightarrow {}^4T_1$ (^4P) give large bands which dominate the absorption spectrum. The absorption spin-forbidden transitions between spin quartet ground state and spin doublet of excited states give sharp bands with low intensity. So, due to the strong crystal field of the host matrix, first excited states of Cr^{3+} doped in α-Al_2O_3 are ^2E, $^2T_1$ states which plays an important role in the emission spectra of ruby. However, in this paper we only analyze the absorption spectrum consisting of transitions from the fundamental state to quartet excited states, allowed by the spin rules. We have carry out all the calculations, based on the methods presented in [24, 25], for three valence chromium ion doped in α-Al_2O_3:Cr^{3+} material using an initial complete active space, consisting of the five-3d metal orbital CAS (3, 5), a good strategy for TM ions doped in host matrices with strongly localized orbitals. The results are collected in tables 1(a) and (b), alongside the experimental data.

For the next step of the calculations we have included the metal-bonding orbitals and electron second d-shell by extending the complete active space to CAS (7, 7), and finally to CAS (7, 12). This procedure improves the reference wave functions and the values of electronic terms energies and, as a consequence the results obtained are more accurate. The results thus obtained are also shown in tables 1(a) and (b). From examining of table 1(a) it can be seen that results from the *ab initio* SORCI and MRDDCI3 methods with CAS(3, 5) reasonably agree with the experimental corresponding values. It should be pointed out that enlarging the active space to
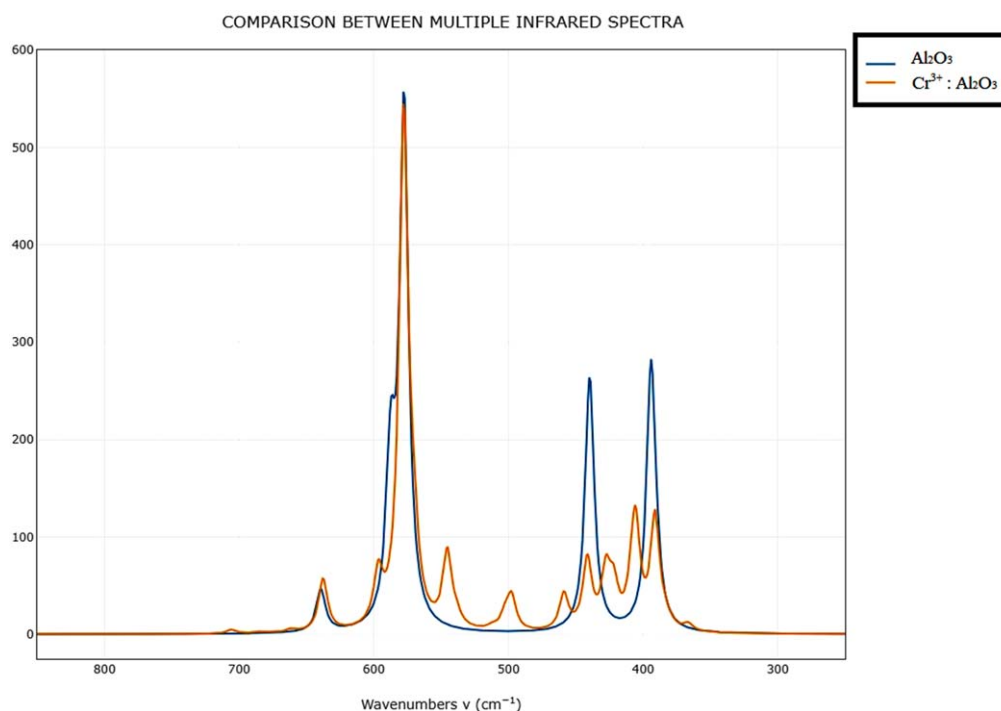
Figure 4. Simulated spectra of α-Al$_2$O$_3$ and α-Al$_2$O$_3$:Cr^{3+}.

Table 6. The calculated and the observed vibrational spectra (cm^{-1}) of α-Al$_2$O$_3$:Cr^{3+}.

Vibration type	IR Exp [54]	IR Calc	Assignment
E	420	422	Cr–O stretching
E	453	459	Al–O stretching
			Cr–O stretching
E	485	498	Cr–O stretching
E	553	545	Cr–O stretching
A	607	597	Cr–O stretching
E	641	638	Al–O stretching
A	782	758	Al–O stretching

CAS (7, 12) the results are improved for transition energies between the ground state ^{4}A$_2$ (^{4}F) and low lying excited spin-doublet states in NEVPT2 method. Concerning the results in tables 1(a) and (b) it need underline that the RMS errors for the case of transitions with forbidden spin rule are larger than in the case of allowed spin transitions. This happen due the more dynamic electronic correlation for high-spin state comparison with the case of low-spin state of d3 electronic configuration and also to the second order perturbation approximation calculations used. On the other hand, based on the results from table 1(a) we have calculated the trigonal ligand field parameters v and v' and collected them in table 2.

Also, the trigonal ligand field parameters together with crystal field parameter Dq allow us to calculate the Wybourne parameters B_{20}, B_{40} and B_{43}.

Furthermore, the g factors have been investigated in the frame of *ab initio* effective spin-Hamiltonian method with QDPT formalism. The results are tabulated in table 3.

Evaluating the data in table 3, we observe a reasonable agreement between the calculated values of the g_{iso} and the experimental data.

A special attention is given to the AILFT procedure in order to obtain the *ab initio* values for the LF splitting parameter 10Dq, the Racah parameters B, C and spin–orbit constant ξ, for both ions, free and doped in corundum crystal. The results are displayed in table 4.

Due to the covalence effect the values of the Racah parameters B, C are smaller than the values B_0 and C_0 of the free chromium ion. Also, for Dq/B and C/B, it can be noted there are larger intervals of variation, depending on the methods used, these are not surprising for *ab initio* calculations on TM ions doped in dielectric host matrices [50].

As can see from table 4 the parameter Dq/B, has different values in the *ab initio* calculations, from small values (1.48-CASSCF, 1.61-NEVEPT2) to more bigger ones (2.10 – DCD-CAS2(0), 2.13-DCD-CAS2(1)). This is possible due because in DCD-CAS2 method we used a Hamiltonian matrix to fit LFT matrix that improves the quality of the fit as compared with NEVPT2, since it includes the possibility of states mixing [42]. As a consequences the LF splitting parameter Dq, in DCD-CAS2 method much closer to the experimental excitation energy of the ^{4}T$_2$ term then the NVPT2 derived parameter. On the other hand the Racah parameters B and C are only slightly changed with respect to NEVPT2. So, the value of the strength of crystal field, defined by Dq/B, calculated with DCD-CAS2 method is superior to that obtained with NEVPT2 method. We underline also, that all *ab initio* values of Dq/B in table 4 are different from the experimental ones. This is because, as is stated in [50], by construction, the ligand field parameters obtained from AILFT are the best possible compromise that guarantees the
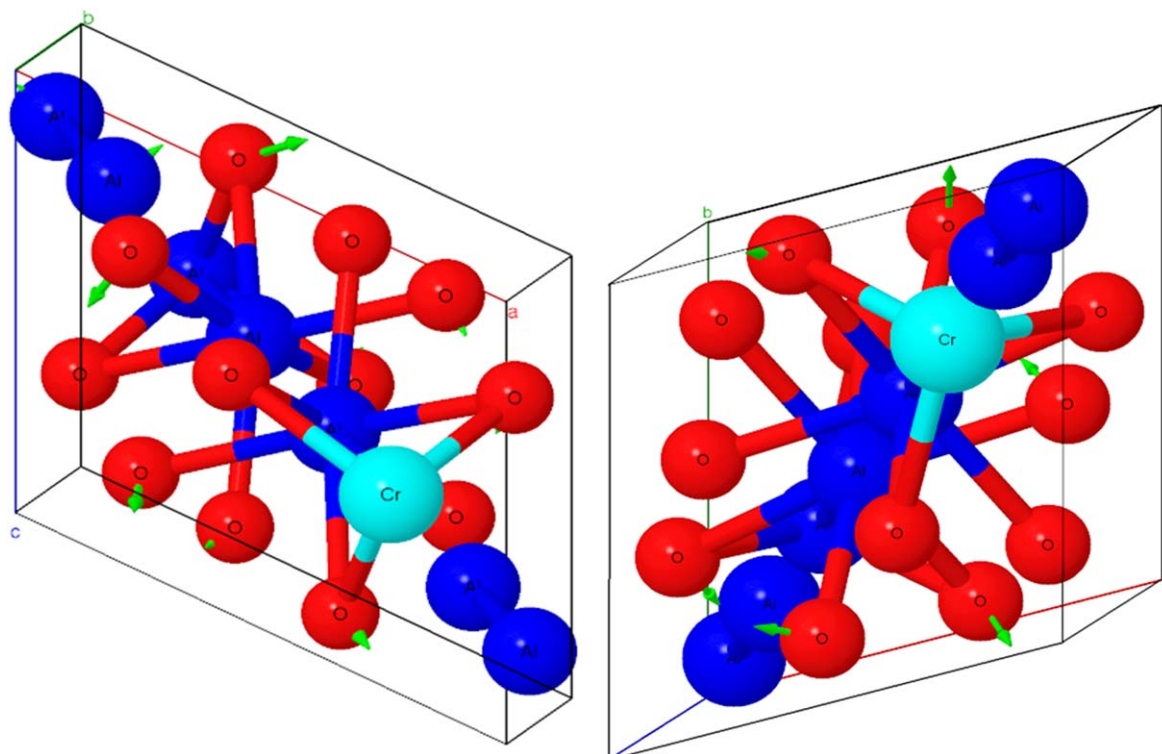
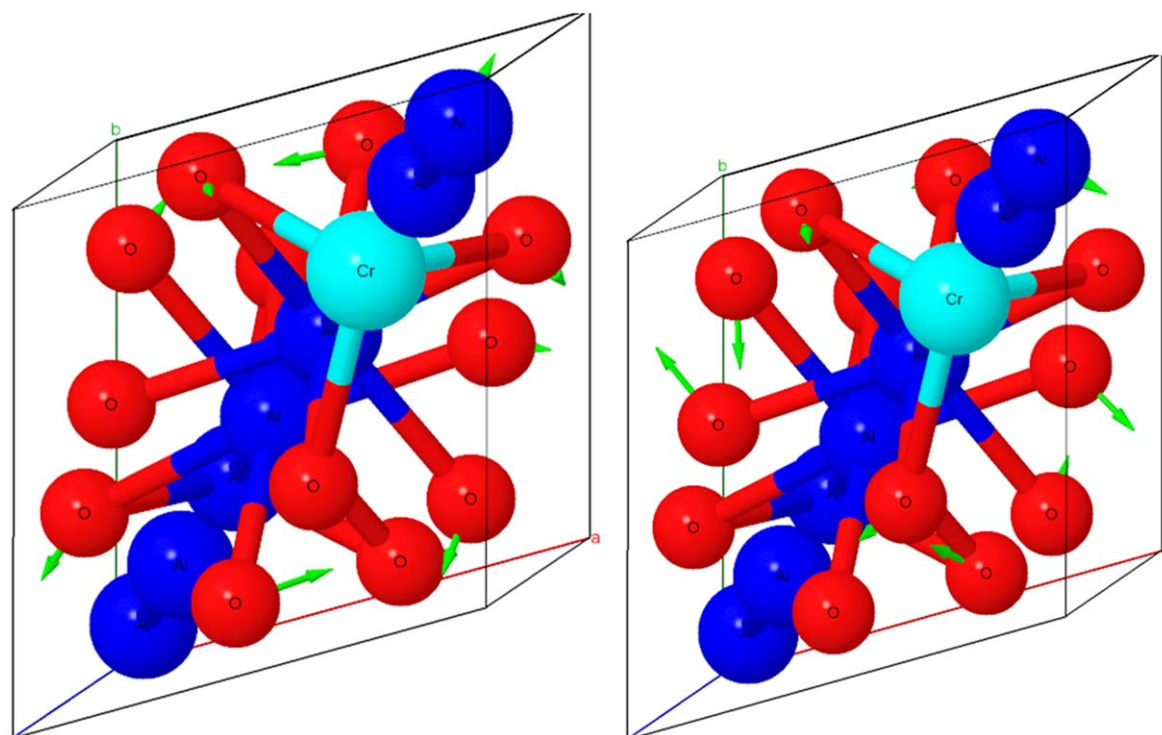**Figure 5.** (a), (b). Vibrational mode Nr 1.

Figure 6. (a), (b) Vibrational mode Nr 2.

closest possible match between ligand field theory and *ab initio* theory for all ligand field states. Contrary, in experimental investigations, one rarely has access to all d–d transition energies, so the empirical fits that determine the values of the ligand field parameters are the subset of states that are actually observed. Using all these parameters we have

recalculated the energy levels by means of the angular overlap program AOMX [48, 49] and the results obtained are compared with the *ab initio* results respectively and with experimental data (see tables 5(a) and (b)).

From tables 5(a) and (b) we can conclude that, as expected, the discrepancies of LFT spectrum from NEVPT2
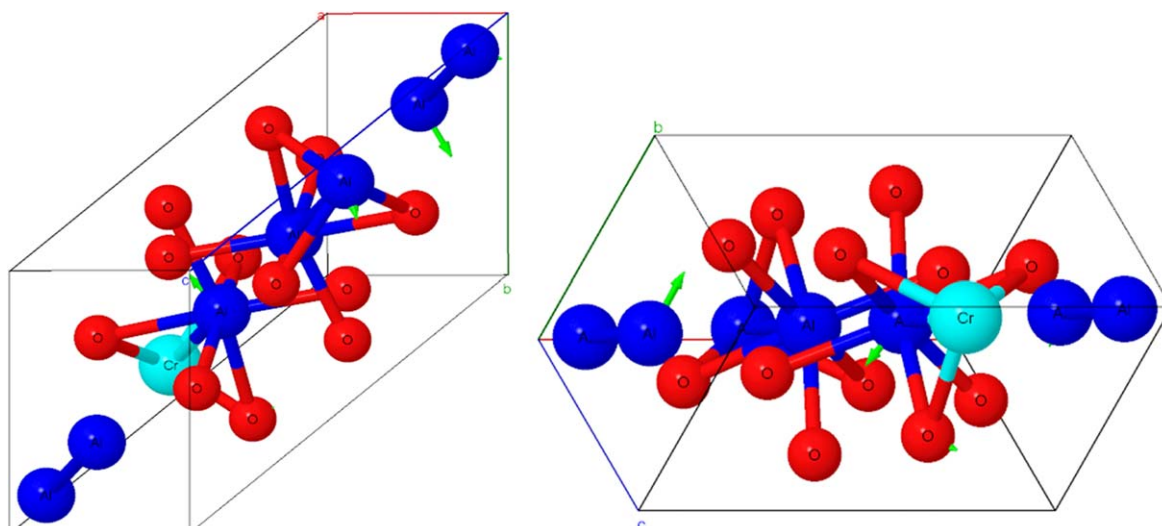
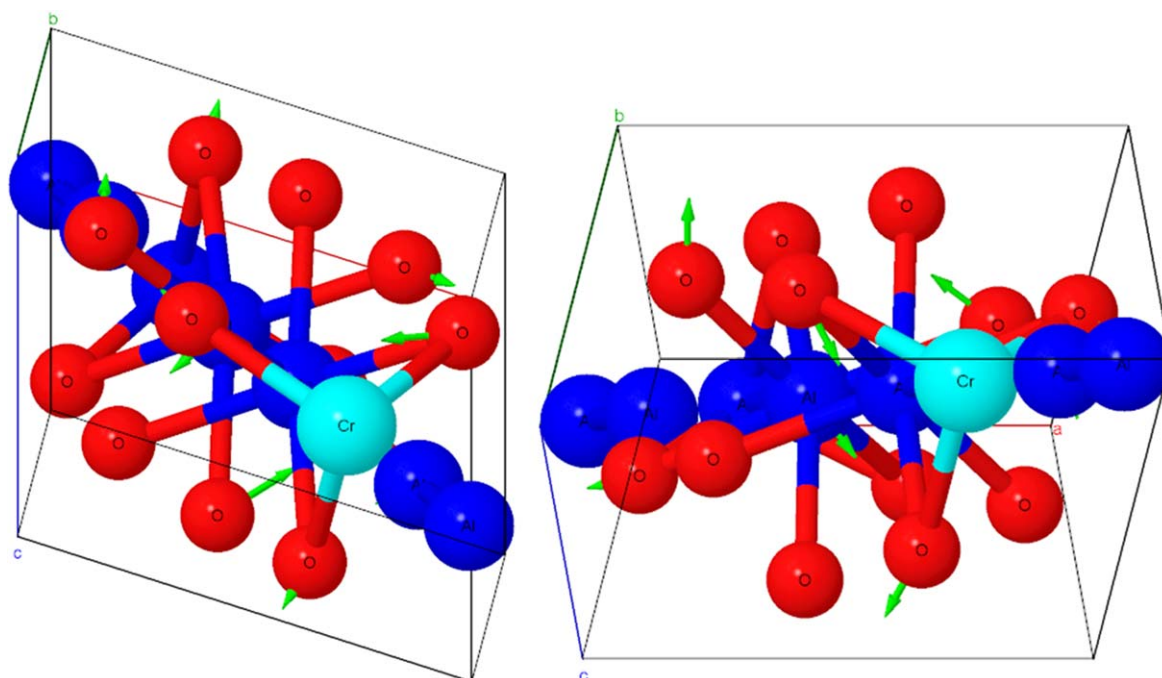**Figure 7.** (a), (b) Vibrational mode Nr 3.

Figure 8. (a), (b) Vibrational mode Nr 4.

are the largest compared to CASSCF results, while the lowest error versus experimental data is obtained with the DCD-CAS2(1) method for spin quartet–quartet transitions and with NEVPT2 method for spin quartet-doublet respectively .

A careful study, briefly presented at the end of this work, based on the lowest stationary point on the potential energy surface, was performed on the vibrational spectra of α-Al$_2$O$_3$ and α-Al$_2$O$_3$:Cr^{3+}. Based on the comparison between the computed and experimental [53] vibrational wavenumbers for pure α-Al$_2$O$_3$, (for brevity this analysis is not given here, but may be provided on request) which are in good agreement and then with values from α-Al$_2$O$_3$:Cr^{3+} FTIR spectrum, the vibrational modes assignment was predicted for each peak.

Finally, we underline that the obtained FTIR spectra contains some strong peaks, due to Al–O and Cr–O stretching bonds (figure 4).

From figure 4 it can be seen that apart from the peaks due to α-Al$_2$O$_3$ host matrix (blue color), the new bands (orange) seen in the spectrum could be assigned as belonging to three valence chromium. The values of wavenumbers corresponding to experimental data [54] and those calculated by us for α-Al$_2$O$_3$:Cr^{3+}crystal are collected in table 6. Additionally, the vibrational modes presented in table 6 were illustrated in figures 5–11 using J-ice [55].

Based on the consistency between the calculated wavenumbers and the experimentally obtained ones, this last study
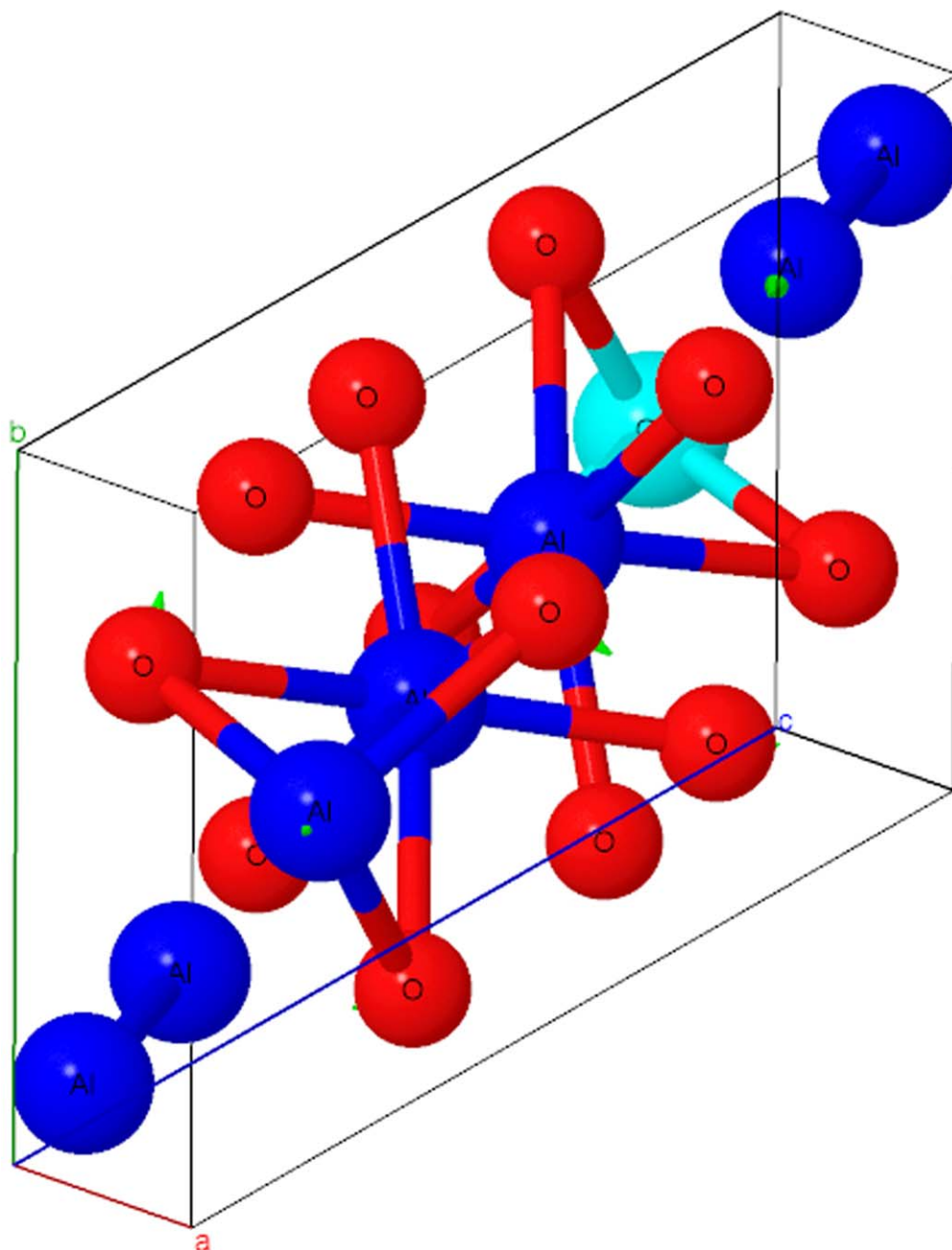
Figure 9. Vibrational mode Nr 5.

certifies the energetically of the created structure by doping trivalent chromium ion in Al_2O_3:Cr^{3+}.

Indeed, the minimum energy achieved in the computed optimized geometry process is also confirmed by the fact that no negative wavenumber modes were obtained.

4. Conclusions

Based on the *ab initio* multireference methods, in the present paper we have calculated, in a unified frame, the positions of the main bands of optical absorption spectra, the ligand field and g factors of α-Al_2O_3:Cr^{3+} crystal. The CASSCF, NEVPT2, DCD-CAS2, MRDDCI3 and SORCI

approximation methods, with CAS (3,5), CAS (7,7) and CAS (7, 12) were used. It has been shown that results carried out by these methods agree well with each other and are also in reasonable agreement with the experimental values. The ligand field parameters Dq, B, C and spin–orbit coupling constant ξ were obtained with the AILFT protocol, implemented in Orca 4.1 software. Moreover, the trigonal parameters v and v' were obtained from quartet energy levels structure and together with the AILFT parameters enables re-calculation of the LFT spectra [48, 49], the analysis of the covalence effects and correlation between the ligands and the structural data of impurity center. The simulated FTIR spectra of the title system confirm the rigorous structure of corundum doped crystal. All the results obtained are in good agreement
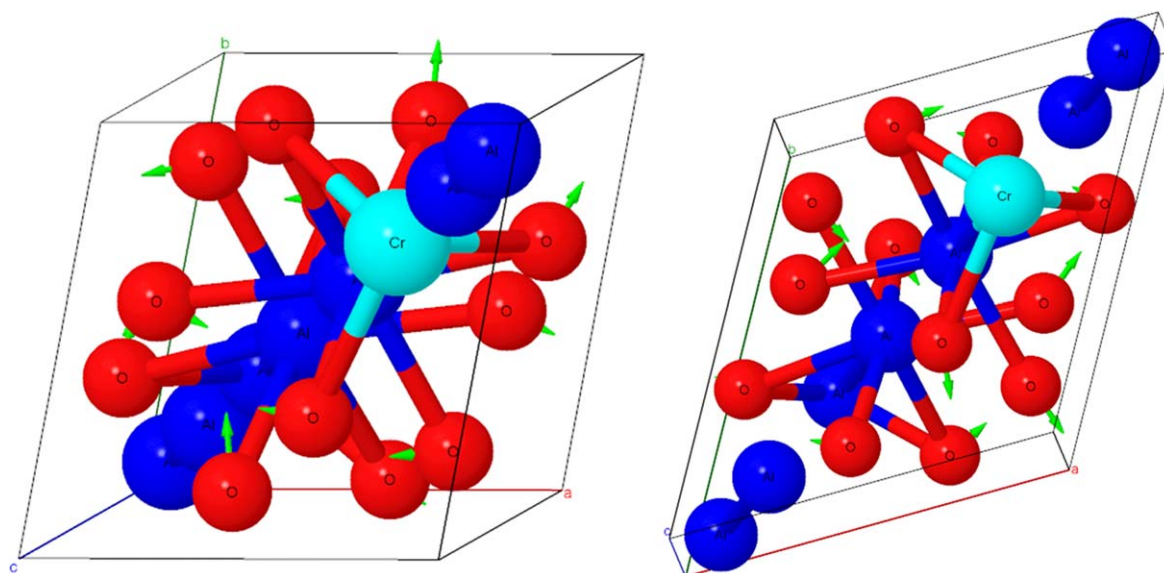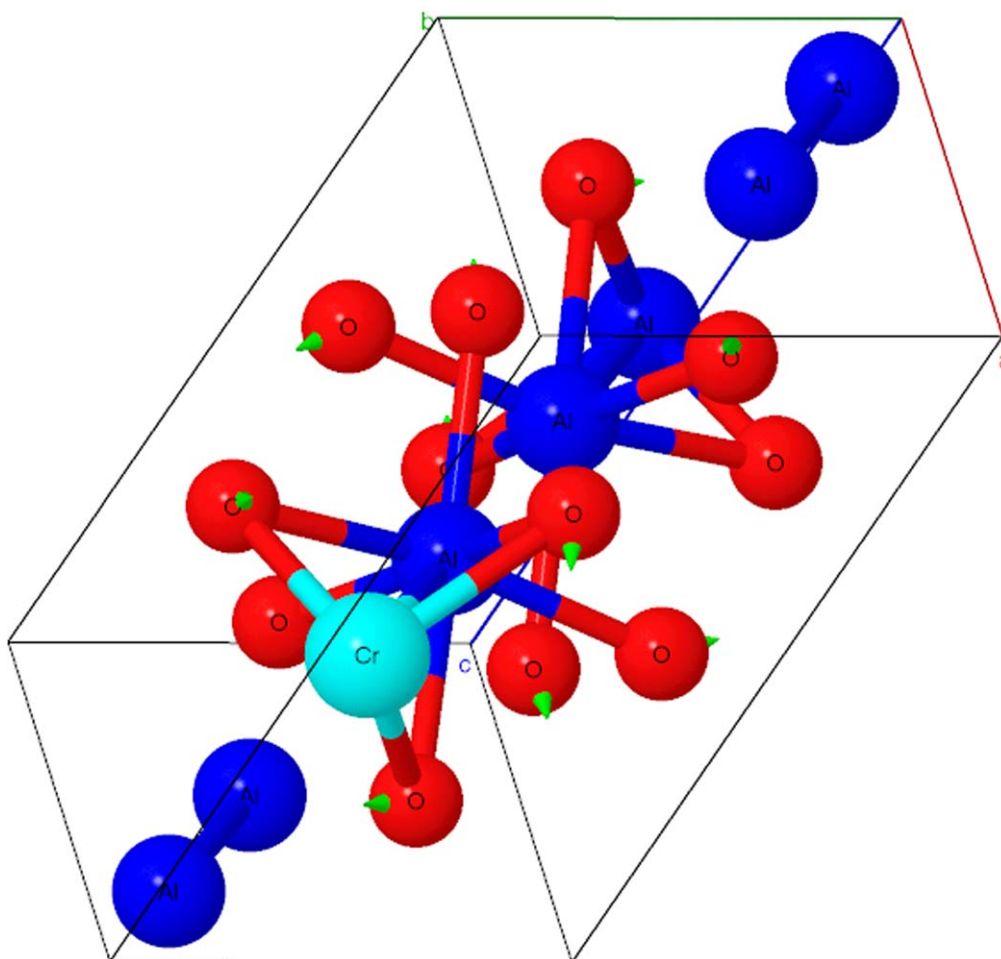
Figure 10 (a), (b) Vibrational mode Nr 6.

Figure 11. Vibrational mode Nr 7.

with those obtained from the *ab initio* methods and the measured data. As expected, through this study, we have gained a better insight of α-Al$_2$O$_3$:Cr^{3+} crystal by means of both *ab initio* and DFT methods.

The *ab initio* multireference methods developed in our earlier publications, applied in this paper for α-Al$_2$O$_3$:Cr^{3+} crystal underlines, once more, its reliability for investigations of the complexes with TM ions. This also allows a deeper

understanding of the d–d transitions of systems with TM doped in host matrices.

Acknowledgments

ORCID iDs

Nicolae M Avram ⓘ https://orcid.org/0000-0001-8848-6380

References

[1] Dellwig T, Rupprechter G, Unterhalt G and Freund H J 2000 *J. Phys. Rev. Lett.* **85** 776
[2] Dörre E and Aluminas H H 1984 *Processing Properties and Applications* (Berlin: Springer–Verlag)
[3] Kim Y, Lee S M, Park C S, Lee S L and Lee M Y 1997 *Appl. Phys. Lett.* **71** 3604
[4] Rousseau D L 1996 *J. Chem. Educ.* **43** 566
[5] Moodera J S, Kinder L R, Wong T M and Meservey R 1995 *Phys. Rev. Lett.* **74** 3273
[6] Powell R C 1998 *Physics of Solid-State Laser Materials* (Berlin, Heidelberg, New York: Springer–Verlag)
[7] Henderson B and Batram R H 2000 *Crystal-field Engineering of Solid-State Laser Material* (Cambridge: Cambridge University Press)
[8] Kück S 2001 *Appl. Phys.* B **72** 515
[9] Toyoda T, Obikawa T and Shigenari T 1998 *Mater. Sci. Eng.* B **54** 33
[10] Trueba A, García-Lastra J M, Garcia-Fernandez P, Aramburu J A, Barriuso M T and Moreno M J 2011 *Phys. Chem.* A **115** 13399–406
[11] Loan T T, Long N N and Ha L H 2011 *e-J. Surf. Sci. Nanotechnol.* **9** 531–5
[12] McClure D S 1962 *J. Chem. Phys.* **36** 2757
[13] Sturge M D 1963 *Phys. Rev.* **130** 639
[14] Tanabe Y and Sugano S 1957 *J. Phys. Soc. Japan.* **12** 556
[15] Fairbank W M Jr, Klauminzer G K and Schawlow A L 1975 *Phys. Rev.* B **11** 60
[16] Sviridov D T, Sviridova R K, Kulik N I and Glasko V B 1979 *J. Appl. Spectrosc.* **30** 334
[17] Novita M and Ogasawara K 2014 *J. Phys. Soc. Japan.* **83** 124707
[18] Brik M G 2018 *Physica* B **532** 178–83
[19] Fang W, Chen H-J, Ma C-G, Zheng W-C, Yang D-X and Gao R-L 2019 *J. Lumin.* **208** 273
[20] Sugano S, Tanabe Y and Kamimura H 1970 *Multiplets of Transition-Metal Ions in Crystals* (New York: Academic)
[21] Salasco L, Dovesi R, Orlando R, Causa M and Saunders V R 1991 *Mol. Phys.* **72** 267
[22] Maiman T H 1960 *Nature* **187** 493
[23] Henderson B and Imbush G F 1989 *Optical Spectroscopy of Inorganic Solids* (Oxford: Clarendon)
[24] Andreici Eftimie E-L, Avram C N, Brik M G and Avram N M 2018 *J. Phys. Chem. Solids* **113** 194
[25] Andreici Eftimie E-L, Avram C N, Brik M G, Chernyshev V A and Avram N M 2019 *J. Lumin.* **214** 0116577
[26] Hahn T 2005 *International Table for Crystallography* vol A (Berlin: Springer)
[27] Momma K and Izumi F 2008 *J. Appl. Crystallogr.* **41** 411272
[28] Newnham R E and de Haan Y M 1962 *Z. Kristallogr.* **117** 234
[29] Dovesi R *et al* 2018 *WIREs Comput. Mol. Sci.* **8** e1360
[30] Perdew J P, Burke K and Ernzerhof M 1996 *Phys. Rev. Lett.* **77** 3865
[31] Gellé A and Lepetit M-B 2008 *J. Chem. Phys.* **128** 244716
[32] Jacob T, Fricke B, Anton J, Varga S, Bastug T, Fritzsche S and Sep W-D 2001 *Eur. Phys. J.* D **16** 257
[33] Neese F 2018 *WIREs Comput. Mol. Sci.* **8** e1327
[34] Reiher M 2005 *Theor. Chem. Acc.* **116** 241
[35] Weigend F and Ahlrichs R 2005 *Phys. Chem. Chem. Phys.* **7** 3297
[36] Kaupp M, Schleyer P V R, Stoll H and Preuss H 1991 *J. Chem. Phys.* **94** 1360
[37] Andrae D, Haeussermann U, Dolg M, Stoll H and Preuss H 1990 *Theor. Chim. Acta* **77** 123
[38] http://theochem.uni-stuttgart.de/pseudopotentials/
[39] Bergner A, Dolg M, Kuechle W, Stoll H and Preuss H 1993 *Mol. Phys.* **80** 1431
[40] Angeli C, Cimirglia R and Malrieu J-P 2002 *J. Chem. Phys.* **117** 9138
[41] Angeli C, Bories B, Cavallini A, Cimirglia R and Malrieu J-P 2006 *J. Chem. Phys.* **124** 054108
[42] Pathak S, Lang L and Neese F 2017 *J. Chem. Phys.* **147** 234109
[43] Miralles J, Castell O, Caballol R and Malrieu J-P 1993 *Chem. Phys.* **172** 33
[44] Neese F 2003 *J. Chem. Phys.* **119** 9428
[45] Malrieu J-P, Caballol R, Calzado C J, de Graaf C and Guihery N 2014 *Chem. Rev.* **114** 429
[46] Atanasov M, Ganyushin D, Sivalingam K and Neese F 2012 *Molecular Electronic Structure of Transition Metal Complexes II* ed D M P Mingos *et al* (Berlin: Springer) pp 149–220
[47] Macfarlane R M 1963 *J. Chem. Phys.* **39** 3118
[48] AOMX a Fortran Program That Calculates d^n Electron Term Energies in the Framework of the Angular Overlap Model Including Electron Interaction and spin–orbit coupling by Adamksy H, based on the AOM1 Program by Hoggard P E, with Contributions by Atanasov M and Eifert K
[49] http://aomx.de/
[50] Singh S K, Eng J, Atanasov M and Neese F 2017 *Coord. Chem. Rev.* **344** 2
[51] Caiut J M A, Floch N, Messadder Y, de Lima O J, Rocha L A, Ciuffi K J, Nasar E J, Fridermann G R and Ribeiro S J L 2019 *J. Braz. Chem. Soc.* **30** 744
[52] Griffith J S 1964 *The Theory of Transition Metal Ions* (Cambridge: Cambridge University Press)
[53] Marshall R, Mitra S S, Gielisse P J, Plendl J N and Mansur L C 1965 *J. Chem. Phys.* **43** 2893
[54] Nguyen D K, Lee H and Kim I T 2017 *Materials* **10** 476
[55] Canepa P, Hanson R M, Ugliengo P and Alfredsson M 2011 *J. Appl. Cryst.* **44** 225–9